Diffuse X-rays from PNe with WR-type central stars

U. Rühling[*,†], C. Sandin[†], M. Steffen[†], D. Schönberner[†], W.-R. Hamann[*] and H. Todt[*]

[*]*Institut für Physik und Astronomie, Universität Potsdam, Germany*
[†]*Astrophysikalisches Institut Potsdam, Germany*

Abstract. With the help of detailed nebula modeling and X-ray observations, we want to shed light on the enigmatic origin of Wolf-Rayet type central stars of planetary nebulae. This method allows us to assign observed [WC] stars to one of the proposed evolutionary scenarios, attributing the loss of hydrogen to a "late", "very late", or an "AGB final" thermal pulse (LTP, VLTP and AFTP, respectively). Following our analysis, we conclude that BD +30° 3639 evolved through an AFTP.

Keywords: hydrodynamics, planetary nebulae: general, planetary nebulae: individual: BD +30° 3639, stars: Wolf-Rayet, X-rays: ISM
PACS: 98.38.Ly

INTRODUCTION

A considerable fraction of all white dwarfs as well as of their progenitors – central stars of planetary nebulae (CSPNe) – shows hydrogen deficient or even hydrogen free surfaces. Depending on the survey, this are 10 to 30 % of the observed objects.

The explanation of the hydrogen loss is not straightforward. Standard evolutionary models predict that a star leaves the AGB before the hydrogen envelope is entirely lost. Thus, the star will move to the hot domain of the HRD while still showing virtually its original surface hydrogen content. [1] described how the hydrogen shell can be mixed down by the very last of the thermal pulses. This last pulse can occur while the star is still on the AGB. In this case, the pulse and the consequent evolutionary scenario are called "asymptotic giant branch final thermal pulse" (AFTP) [2]. However, the star can also experience the last pulse while the star has already left the AGB. Hence, the last thermal pulse can occur when the star is a CSPN or even while it is on the white dwarf cooling branch. Consequently, the pulse forces the star's envelope to expand rapidly back to AGB dimensions. These cases are called "late thermal pulse" (LTP) [3] or "very late thermal pulse" (VLTP) [1] and lead to a "born-again" scenario.

In case of an AFTP, the fast central-star wind that sweeps up the nebula is hydrogen deficient from the beginning. The wind energy powers a hot bubble within the the optical nebula that shows a CO-enriched X-ray spectrum. In a born-again scenario on the other hand, the last thermal pulse occurs after a hydrogen-rich stellar wind had already swept up the nebula. Consequently, the X-ray emitting region is expected to be located closer to the central star, showing the predicted LTP/VLTP abundances. The two scenarios are sketched in Fig. 1. We will perform detailed hydrodynamical model calculations of the nebula with the NEBEL code [4]. Parameter studies will provide more discriminating

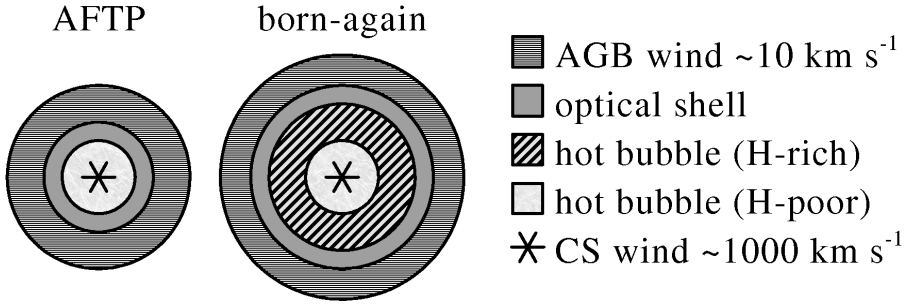

FIGURE 1. Cartoon of the X-ray emitting region in an AFTP/ born-again scenario. Not to scale.

criteria.

As a first case, we will try to model BD +30° 3639. Due to its relatively small distance of 1.2 kpc [5], it has the X-ray brightest nebula of all [WC]-type central stars. Hence, it was possible to secure a high-resolution X-ray spectrum [6]. BD +30° 3639 has a relatively cool late-type ("[WCL]") central star with $T_{\rm eff} = 47$ kK [7]. With a radius of 4.0 arcsec, the nebula is not very extended. Since its kinematic age is about 800 yr [5], a born-again scenario is not expected for this object. With NEBEL modeling, we will test the hypothesis of an AFTP scenario. The following sections will give a status report of the on-going work.

X-RAY OBSERVATIONS

Planetary nebulae have been identified as weak, diffuse X-ray sources. Four PNe with [WC]/[WO] central stars have been detected in X-rays, in addition to the nebula of the hydrogen-deficient star A 30 (of type "wels") [6, 8, 9, 10, 11]. Recently, we added another X-ray observation of A 30 with XMM-Newton (PI: Hamann). There are only few non-detections of PNe with hydrogen deficient central stars. Three of them are PG1159 stars. The non-detection of Hen 2-99 ([WC9]) can be explained by its low age – it might be too young to have formed a hot bubble [8]. All observed X-ray temperatures are around a few 10^6 K. There is no obvious difference to the X-ray temperatures observed for PNe with hydrogen-normal nuclei [12].

For PNe with hydrogen-normal central stars, the X-ray emission has been explained with hydrodynamical models [13]. The AGB wind of $\sim 10\,{\rm km\,s^{-1}}$ provides the "initial condition" of the evolutionary nebula model. The following fast CSPN wind ($\sim 1000\,{\rm km\,s^{-1}}$) collides with the much denser and slower nebular gas and becomes shocked. Between the contact discontinuity and the reverse shock a hot bubble arises. This bubble is heated to some 10^7 K with very low electron density and hence low X-ray emissivity. Thermal conduction between the cool, dense optical shell and the hot bubble decreases the temperature to the observed few 10^6 K and increases the electron density and the emissivity. As PNe with [WC] type central stars show the same temperatures, we expect that heat conduction plays an equally important role in the temperature-determining processes (see section on nebula modeling). Additional evidence for this model is given by the observation that X-rays are preferably detected from PNe with

closed rims [11]. Furthermore, two of the objects are resolved well enough to exhibit limb brightening: NGC 40 and NGC 6543 [8, 14], which is predicted by the models of [13].

STELLAR WIND MODELING

The energy that powers the hot bubble is converted from the mechanical energy of the stellar wind. Thus, the mass-loss rate and the terminal wind velocity are important input parameters for the nebula models. State-of-the-art parameters can be determined from spectral analysis with PoWR, the Potsdam Wolf-Rayet model atmosphere code [15, 16]. The code simulates spectra for spherically symmetric expanding atmospheres. It adequately treats the supersonic motion and extreme deviations from local thermodynamical equilibrium ("non-LTE"). Line transitions between many levels of different ions of abundant elements have to be taken into account. Altogether, a few thousand line transitions (typically of H, He, C, N, O) are treated explicitly, and many million additional line transitions (of the iron-group elements) in a slightly approximate way (by "superlevels"). The stellar parameters are the effective temperature, luminosity, radius, mass-loss rate and terminal wind velocity. In all atmosphere calculations discussed in this work, the stellar wind is semi-empirically parameterized but not derived from self-consistent hydrodynamics.

The main uncertainty in the determined mass-loss rate comes from the degree of clumping in the wind, which is subject of current debates [17]. Here we will discuss only the terminal velocity as an input parameter for the NEBEL code. The terminal velocity is measured from the line widths. The terminal velocity of BD $+30^\circ$ 3639 was determined to be $700\,\mathrm{km\,s^{-1}}$ [7] (see Fig. 2, left panel). However, this velocity is too small to form a hot X-ray emitting bubble because gas cooling by lines is very efficient for a hydrogen-free plasma [18]. The P-Cygni profiles indicate a higher terminal velocity (Fig. 2, right panel). Measurements of UV P-Cygni lines give $850\,\mathrm{km\,s^{-1}}$ (FUSE) and $1000\,\mathrm{km\,s^{-1}}$ (IUE, very noisy spectra) [19]. For all WR stars, the velocities measured from the blue edge of the UV P-Cygni profiles tend to be systematically higher than the velocities measured from optical emission lines.

This discrepancy between optical emission lines and UV P-Cygni profiles probably has two reasons: The assumed velocity field (the so-called "β-law") might only hold well for the inner region of the wind where the optical emission lines arise from, but might not be a good assumption for regions far out in the wind where the blue edges of P-Cygni absorption lines are formed. The other reason might be turbulence. Not only the average turbulence velocity, but probably its maximum value has to be added to the terminal wind velocity to reproduce the shift of the blue edge of strong P-Cygni profiles. Microturbulence is a free parameter of the models which is set to $100\,\mathrm{km\,s^{-1}}$ by default. Subtracting this value from the $850\,\mathrm{km\,s^{-1}}$ measured from FUSE P-Cygni profiles would give the old terminal velocity of $\sim 700\,\mathrm{km\,s^{-1}}$. Marcoturbulence is not treated in the PoWR code, but it can also add to the blue edge of the P-Cygni profiles. Neither micro- nor macroturbulence are considered in the NEBEL code.

The NEBEL code models the evolution of the nebula starting from the AGB star wind. Hence, not only the parameters of the current star, but also of its likely progenitors

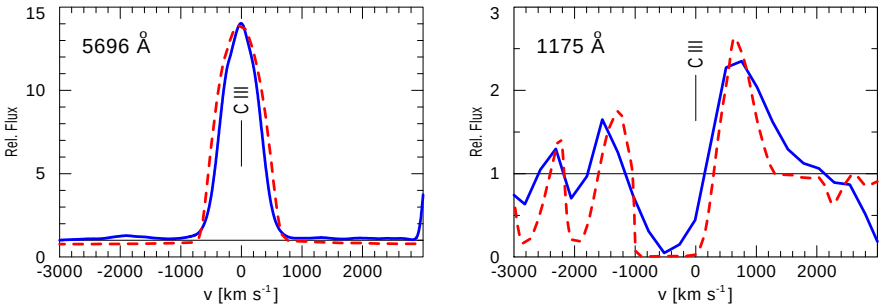

FIGURE 2. Spectrum of BD +30° 3639. Blue: observation. Red dashed line: PoWR model with $v_\infty = 700\,\mathrm{km\,s^{-1}}$.

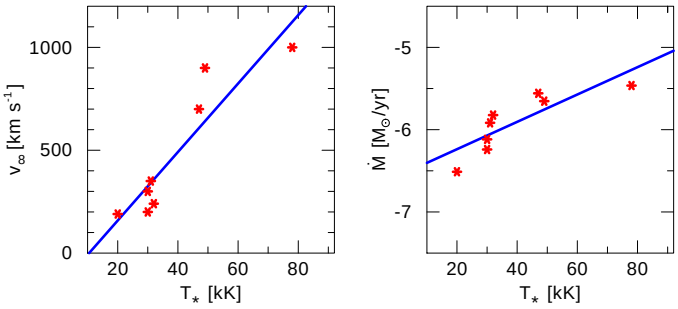

FIGURE 3. Terminal velocity (left) and mass-loss rate (right) over effective temperature for a sample of [WCL] stars by [20].

are needed. In Fig. 3, velocity measurements of a sample of [WCL] stars by [20] are plotted over the stellar effective temperature. Since the stellar temperature rises with the evolutionary age, it serves as its proxy. The stars in this sample with temperatures down to 20 kK are considered as progenitor templates for BD +30° 3639 in the NEBEL code. Their terminal wind velocities increase with age. The same relation is shown for the mass-loss rate.

NEBULA MODELING

We model the nebulae with a 1-D hydrodynamical code, accounting for the evolution of the stellar wind of [WC]-type central stars as depicted in Fig. 1. Previous models taking heat conduction into account were assuming a pure hydrogen plasma for simplicity [13]. This assumption cannot be sustained for a hydrogen deficient wind. To adequately model heat conduction in a WR wind formed bubble, we implemented an extended description of heat conduction. The general Fokker-Planck-based theory by [21] also works for other compositions. Since the Chapman-Enskog-Burnett version of the theory of [22] (and references therein) differs only very little in the results, we chose the simpler Fokker-Planck formulae. Hence, for the first time, the models include a description of heat conduction in a hydrogen-poor plasma.

We can report preliminary results. The heat conduction in a hydrogen poor plasma is

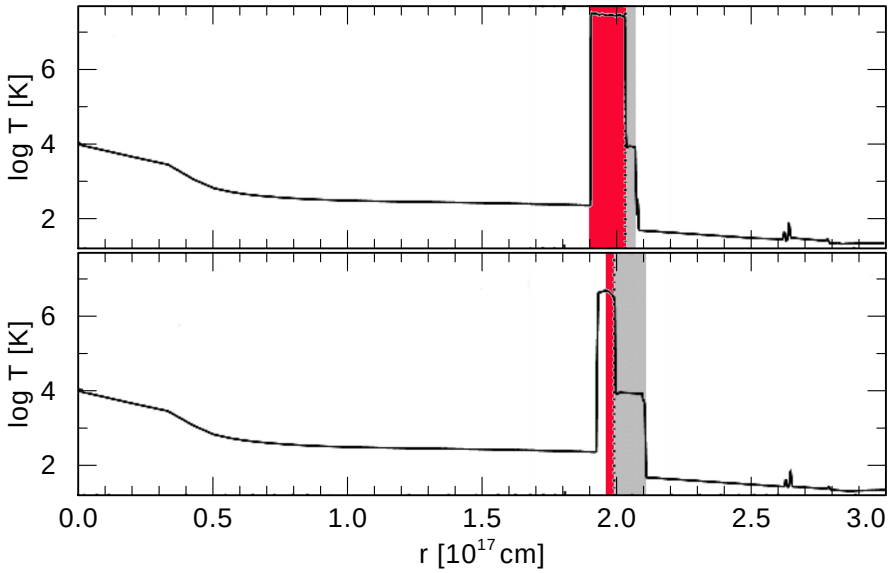

FIGURE 4. Temperature profile of the nebula. Upper panel: without heat conduction. Lower panel: with heat conduction. Dark red: hot bubble. Light gray: optical nebula.

less efficient. The diffusion coefficient is about two times lower than in a plasma where only hydrogen nuclei limit the free path of the free electrons. Nevertheless, the process is powerful enough to cool the hot bubble. The upper panel in Fig. 4 shows the temperature profile of a NEBEL model based on an evolutionary track with no born-again scenario and without heat conduction. The hot bubble shows a temperature of $T_{\rm X} > 10^7$ K. Considering heat conduction of the hydrogen-poor plasma, the temperature drops to the observed $1.7 - 2.9 \cdot 10^6$ K [6]. Furthermore, the electron density close to the contact discontinuity rises from $n_{\rm e,bubble} < 10\,{\rm cm}^{-3}$ (no heat conduction) to $n_{\rm e,bubble} \sim 50\,{\rm cm}^{-3}$. Without heat conduction, the bubble forms early and close to the star and occupies a large volume. Taking heat conduction into account, the bubble forms later and in a thiner nebula shell (see Fig. 4).

The model was calculated using BD +30° 3639 parameters. However, the position and size of the hot bubble do not fit with the observations. Currently, we are calculating a series of models of this object, testing the influence of all input parameters. These models will be published and discussed in a subsequent paper.

We calculated also the X-ray spectrum for the current models using the CHIANTI atomic database (version 6.0.1). Some of the lines observed by [6] are indicated. The line ratio O VIII(18.967)/O VII(18.627) ~ 2 compares well with the ratio observed for the case with heat conduction.

PRELIMINARY RESULTS

Different indicators point to an AFTP evolution in the case of BD +30° 3639. As stated above, the nebula is young and not very extended. Furthermore, the observed X-ray plasma abundances by [6] are consistent with current hydrogen-free wind abundances as

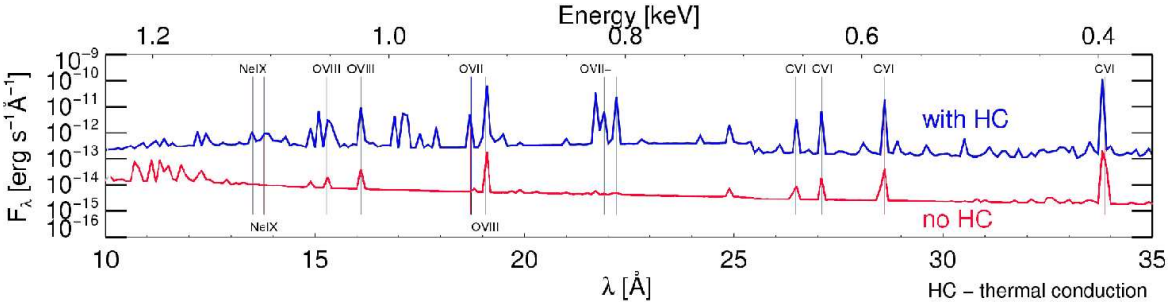

FIGURE 5. Predicted X-ray spectrum for the both cases shown in Fig. 4.

determined by [7]. Due to the small nebula extension, the X-ray emission is not spatially resolved well enough to determine if the hot bubble exactly fills the optical nebula or if the bubble shows limb brightening. A counter-argument to the AFTP hypothesis is given by the observed stellar chemical abundances. The hydrogen-free abundances as found by [7] do not match the AFTP evolutionary calculations by [2] who predict that some hydrogen should be left over. Preliminary results from our modeling of the nebular evolution indicate that BD +30° 3639 is consistent with the AFTP scenario. The NEBEL model considering heat conduction shows X-ray emission of $2 \cdot 10^6$ K as observed. Even though the model cannot yet be considered as a fit, we are optimistic to achieve it soon.

REFERENCES

1. F. Herwig, T. Blöcker, N. Langer, and T. Driebe, *A&A* **349**, L5–L8 (1999).
2. F. Herwig, "Stellar Evolution and Nucleosynthesis of Post-AGB Stars," in *Astrophysics and Space Science Library*, edited by R. Szczerba & S. K. Górny, 2001, vol. 265 of *Astrophysics and Space Science Library*, p. 249.
3. L. G. Althaus, A. M. Serenelli, J. A. Panei, A. H. Córsico, E. García-Berro, and C. G. Scóccola, *A&A* **435**, 631–648 (2005).
4. M. Perinotto, D. Schönberner, M. Steffen, and C. Calonaci, *A&A* **414**, 993–1015 (2004).
5. J. Li, J. P. Harrington, and K. J. Borkowski, *AJ* **123**, 2676–2688 (2002).
6. Y. S. Yu, R. Nordon, J. H. Kastner, J. Houck, E. Behar, and N. Soker, *ApJ* **690**, 440–452 (2009).
7. W. L. F. Marcolino, D. J. Hillier, F. X. de Araujo, and C. B. Pereira, *ApJ* **654**, 1068–1086 (2007).
8. R. Montez, Jr., J. H. Kastner, O. De Marco, and N. Soker, *ApJ* **635**, 381–385 (2005).
9. R. A. Gruendl, M. A. Guerrero, Y. Chu, and R. M. Williams, *ApJ* **653**, 339–344 (2006).
10. Y. Chu, T. H. Chang, and G. M. Conway, *ApJ* **482**, 891 (1997).
11. J. H. Kastner, R. Montez, Jr., B. Balick, and O. De Marco, *ApJ* **672**, 957–961 (2008).
12. M. A. Guerrero, Y. Chu, and R. A. Gruendl, "The X-ray Planetary Nebulae Database," in *The X-ray Universe 2005*, edited by A. Wilson, 2006, vol. 604 of *ESA Special Publication*, p. 85.
13. M. Steffen, D. Schönberner, and A. Warmuth, *A&A* **489**, 173–194 (2008).
14. Y. Chu, M. A. Guerrero, R. A. Gruendl, R. M. Williams, and J. B. Kaler, *ApJL* **553**, L69–L72 (2001).
15. G. Gräfener, L. Koesterke, and W. Hamann, *A&A* **387**, 244–257 (2002).
16. W. Hamann, and G. Gräfener, *A&A* **427**, 697–704 (2004).
17. W. Hamann, L. M. Oskinova, and A. Feldmeier, "Spectrum formation in clumpy stellar winds," in *Clumping in Hot-Star Winds*, edited by W.-R. Hamann, A. Feldmeier, & L. M. Oskinova, 2008, p. 75.
18. G. Mellema, and P. Lundqvist, *A&A* **394**, 901–909 (2002).
19. M. A. Guerrero, G. Ramos-Larios, and D. Massa, *PASA* **27**, 210–213 (2010).
20. U. Leuenhagen, W. Hamann, and C. S. Jeffery, *A&A* **312**, 167–185 (1996).
21. L. Spitzer, *Physics of Fully Ionized Gases*, 1962.

22. R. S. Devoto, *Physics of Fluids* **10**, 2105–2112 (1967).